Computer-Aided Formation of the Whole-Cell Patch-Clamp Recording Configuration

P. Novák and I. Zahradník

Institute of Molecular Physiology and Genetics, Slovak Academy of Sciences, Bratislava, Slovakia. E-mail: pavel.novak@savba.sk

Abstract. The conventional patch-clamp technique requires well-trained experimenter. Few commercial automated patch-clamp systems, designed for drug development, are better suited for large-scale research then for standard electrophysiological experiments. Here we describe a state machine for automated recognition of recording states of the patch-clamp experiment. The principle of the state machine is based on evaluation of the charge carried by membrane current during specific time segments in responses to square wave voltage stimulation. The state machine may serve for generating various sound alerts, signals for automated control of other devices, assistance in micromanipulation, internal pipette pressure control, and holding potential adjustments. Algorithm of the state machine, designed to cover wide variety of cell types, was successfully tested on rat ventricular myocytes.

Key words: Patch-clamp — Automation — Cardiac myocytes

Introduction

Invention of the patch-clamp technique (Hamill et al. 1981) defined a new standard in studies of passive and active electrical characteristics of cells. While offering unbeatable resolution and versatility, the whole-cell patch-clamp technique ranks among the most labor-intensive techniques suffering from low throughput and high demands on experimenters. To simplify the use of patch-clamp technique and to increase its throughput, a number of different automated patch-clamping systems have been developed utilizing novel planar-electrode technology (Fertig et al. 2002; Klemic et al. 2002; Stett et al. 2003; Asmild et al. 2003) or modified glass-pipette technology (Leppe-Wienhues et al. 2003). Most of these systems were designed primarily as high-throughput screening tools for drug development, leaving the basic research-oriented patch-clamp studies on well-trained experimenters. Reports describing individual automation techniques in detail, such as the control of patch-

Correspondence to: Ivan Zahradník, Institute of Molecular Physiology and Genetics, Slovak Academy of Sciences, Vlárska 5, 833 34 Bratislava 37, Slovakia
E-mail: ivan.zahradnik@savba.sk

pipette internal pressure in conventional patch-clamp (Heyward and Shipley 2003), with respect to basic research are very rare.

The aim of this work was to design system that would assist experimenters to obtain whole-cell recording configuration and so would reduce workload on the experimenter. We describe a system for automatic recognition of individual patch-clamp states, starting with the pipette positioned above the level of the bath solution and ending with formation of the whole-cell patch-clamp configuration. The principle of automatic recognition is based on measurement of charge in specific time segments of current response to square wave stimulation. Once an automatic recognition of current state of patch-clamp recording configuration is available, it is possible to generate various control signals, e.g., for the z-drive of the micromanipulator, for the intensity and polarity of the pressure applied to the patch-pipette, or for the value of applied holding potential, and thus it is possible to automate establishing of the whole-cell patch-clamp configuration. With this system, the experimenter only has to position the pipette tip right above the cell, unless a separate machine-vision system capable of locating cell is available as in the Apatchi-1^{TM} system (Asmild et al. 2003).

Materials and Methods

Cell preparation and solutions

The experiments were performed in accordance with the guidelines laid down by the Slovak Academy of Sciences animal welfare committee. Myocytes were isolated enzymatically from left ventricles of male Wistar rats (200–250 g) as previously described in Zahradnikova et al. (2004). Experiments were performed at room temperature (22–23°C). The standard bath solution contained (in mmol/l): 135 NaCl, 5.4 CsCl, 1 $CaCl_2$, 5 $MgCl_2$, 0.33 NaH_2PO_4, 10 HEPES (pH 7.3). The composition of the pipette solution was (in mmol/l): 135 $CsMetSO_3$, 10 CsCl, 1 EGTA, 3 $MgSO_4$, 3 Na_2ATP, 0.05 cAMP, 10 HEPES (pH 7.1).

Electrophysiology

Measurements were made using the Axopatch 200B patch-clamp amplifier (Axon Instruments Inc., Union City, CA). Current output was low-pass filtered by the Axopatch 200B built-in 10–100 kHz 8-pole Bessel filter, and digitized at 100 kHz by 16-bit data acquisition system Digidata 1320A (Axon Instruments Inc., Union City, CA). Square wave voltage stimuli were generated by the Digidata 1320A 16-bit D/A converter.

Definition of individual states leading to the whole-cell configuration

To achieve a working whole-cell configuration, the recording state has to go through several phases (Hamill et al. 1981). The whole procedure starts with the pipette tip above the bath level positioned right above the cell selected for patch-clamping. In this state, dubbed here as “In air”, the current response is flat with very short

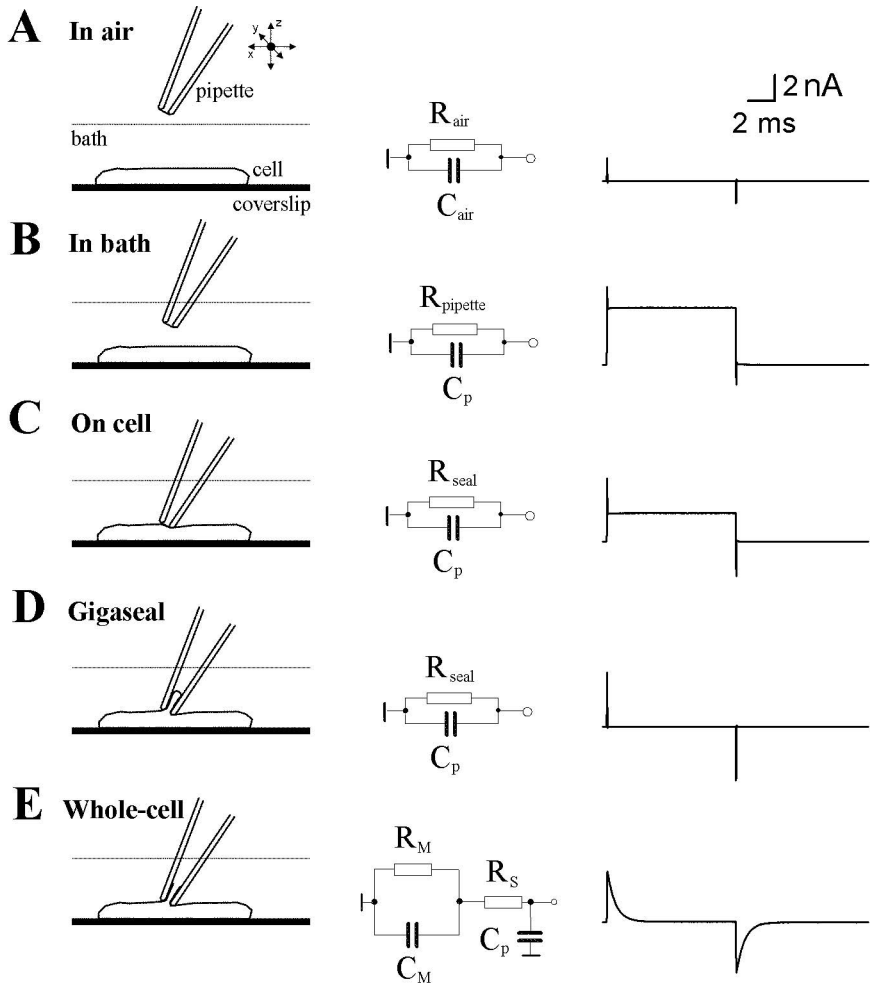

Figure 1. Establishing the whole-cell recording configuration. The whole procedure of preparing the whole-cell configuration is decomposed into 5 states: "In air" (A), "In bath" (B), "On cell" (C), "Gigaseal" (D) and "Whole-cell" (E). The left column illustrates position of the patch-pipette with respect to the cell and the bath solution in a given state. Mutual arrangement of the pipette, cell membrane and the bath results in equivalent electrical circuits shown in the middle column, and, in a typical current responses to the square wave voltage stimulation illustrated in the right column. The equivalent circuits consist of two elements with the resistive element describing the resistance in the air R_{air} (A), the resistance of the patch-pipette R_{pipette} (B) or the resistance of the seal between the membrane and the pipette R_{seal} (C and D) and the capacitive element describing the capacitance over the air C_{air} (A) or the capacitance of immersed part of the pipette C_{P} (B–D). In the "Whole-cell" configuration the number of elements in the equivalent circuit increases to four with the membrane resistance R_{M}, the membrane capacitance C_{M}, the series resistance R_{S} (E) and the parasite capacitance C_{P}.

transients resulting from uncompensated parasite capacitance ower the air C_{air} (Fig. 1A). A positive pressure has to be applied to the pipette to preserve clean surface of the tip when proceeding to the next state, referred to here as "In bath" (Fig. 1B). Immersion of the pipette in the bath is characterized by a sudden change from the flat current response to a square wave current response with the amplitude inversely proportional to the pipette resistance R_{pipette} (Fig. 1B). Next, experimenter manipulates the pipette to the cell surface and gently pushes against the membrane of the cell using the z-drive of micromanipulator, until the resistance of the seal R_{seal} reaches the user-defined multiple of the R_{pipette}. The recording state is now "On cell" (Fig. 1C). From now on, the membrane patch located below the pipette tip is pulled inside the pipette by applying a negative pressure to the pipette (and negative holding voltage if required), until a "Gigaseal" state is reached. The "Gigaseal" state is defined as the state with R_{seal} above the user-defined minimum value (Fig. 1D). The pipette pressure can be released to allow the seal to stabilize and to set the resting potential for the given cell prior to rupturing the membrane patch by small pulses of negative pressure or by voltage pulses (zapping) applied to the pipette. Rupture of the membrane patch forms a direct electrical contact of the pipette with the internal space of the cell. This "Whole-cell" state is indicated by the appearance of exponentially decaying current response (Fig. 1E).

Current responses can be analyzed using various built-in tools and routines of any commercially available data acquisition and analysis software. However, the selection of a proper analysis tool along with a proper voltage stimulus amplitude, duration, and holding level, required for the recording state of interest, is left upon the experimenter, since the software itself keeps no information about the recording state. A system for automatic recognition of the recording state would greatly reduce interactions of the user with the software. Additionally, it will allow automatic analysis and automatic control of external devices used during experiments.

Principle of automatic recording state recognition

When ignoring the parasite capacitance, there are only two types of current responses throughout the whole process of making the whole-cell configuration – the square wave responses with amplitudes ranging from several nA to virtually zero, and the exponentially decaying current responses. Therefore the basic task of the automatic recognition system is to distinguish between the square wave and exponential wave responses. In principle, the type of current response can be estimated by several methods, for example, by comparing the peak and steady state current values or by approximating the current response by an exponential function. However, most of these approaches would led to serious problems in practical applications, for instance due to random spikes, aliasing, divergence of exponential fit, computation efficiency etc. We solved this problem by developing a robust and straightforward procedure insensitive to current variations in experiment.

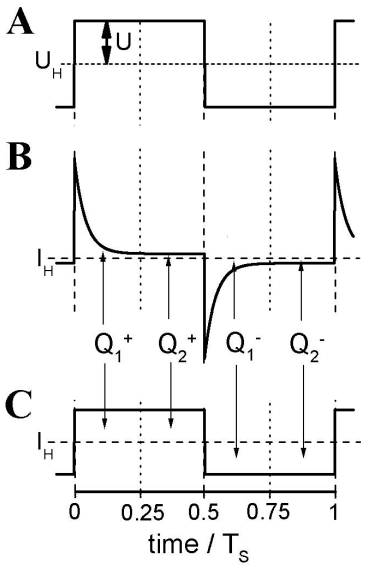

Figure 2. The principle of automatic recognition. When a square wave voltage stimulus of amplitude U superimposed on the holding potential U_{H} and of period T_{S} (A) is applied to the patch-pipette, the current response has a form of a square waves (C) before, and the form of an exponential waves (B) after formation of the whole-cell configuration. These two types of the responses can be distinguished very simply by comparing the charges Q_1^+, Q_1^- and Q_2^+, Q_2^- obtained by integration of the current response within the time segments of $T_{\mathrm{S}}/4$ duration, indicated by vertical dotted and dashed lines. Obviously, the ratio of Q_1 and Q_2 charges in the exponential wave is different than in the square wave type of response.

Assuming a bipolar square wave voltage stimulus with amplitude of $\pm U$ and period T_{S} (Fig. 2A), the ideal exponential and square wave responses can be distinguished simply by evaluating the ratio F (fraction):

$$F = \frac{Q_1}{Q_2} \tag{1}$$

where Q_1 and Q_2 are charges calculated from integration of the current response $i(t)$ within segments of $T_{\mathrm{S}}/4$ duration (Fig. 2B):

$$Q_1 = \frac{1}{2}\left[\int_0^{T_{\mathrm{S}}/4} i\,(t)\,\mathrm{d}t - \int_{T_{\mathrm{S}}/2}^{3T_{\mathrm{S}}/4} i\,(t)\,\mathrm{d}t\right] = \frac{Q_1^+ - Q_1^-}{2} \tag{2}$$

$$Q_2 = \frac{1}{2}\left[\int_{T_{\mathrm{S}}/4}^{T_{\mathrm{S}}/2} i\,(t)\,\mathrm{d}t - \int_{3T_{\mathrm{S}}/4}^{T_{\mathrm{S}}} i\,(t)\,\mathrm{d}t\right] = \frac{Q_2^+ - Q_2^-}{2} \tag{3}$$

Ideally, the ratio F is 1 for the square wave, and greater than 1 for exponential response. In practice, a small number of samples just after the onset of the current response containing the fast transient due to uncompensated parasite capacitance C_{P} (typically 60–70 μs at 10 kHz low-pass filtering) have to be excluded from the calculation of Q_1 and Q_2 to prevent the "Gigaseal" or "In air" states from being misinterpreted as the "Whole-cell" configuration. Even then there's a risk of confusion between "Gigaseal" and "Whole-cell" due to noise and hum in the

current response, which in combination with very low values of Q_1 and Q_2 in the "Gigaseal" may result in the ratio F reaching values larger than 1. Therefore, we defined a minimal value of the ratio $F \geq 3$ and the minimal value of the membrane charge $Q_1 - Q_2 \geq 50$ fC to safely acknowledge estimation of the current response as the exponential decay type, i.e., of the true "Whole-cell" state.

Eqs. (1–3) serve for basic differentiation between the final "Whole-cell" state with exponential response and all preceding states exhibiting square wave response. Precise identification of individual states prior to the final "Whole-cell" is based on the knowledge of the correct sequence of states and on the estimation of the resistive part R_X of their equivalent circuits (where X stands for pipette, seal or air, Fig. 1A–D):

$$R_X = \frac{UT_S}{2\,(Q_1 + Q_2)} \tag{4}$$

The knowledge of the correct sequence helps in identifying states with similar values of R_X, as for example the "Gigaseal" and "In air". If the current value of R_X is of the order of GΩ and the previous state was "On cell", than the current state cannot be "In air", but "Gigaseal".

Setting the stimulus period for optimal exponential response recognition

Successful identification of exponential response according to the algorithm described above depends on the stimulus period T_S. When the stimulus period is too long compared to the time constant of the whole-cell configuration τ, the charge accumulated on the membrane $(Q_1 - Q_2)$ is low compared to charge Q_2 and the ratio F is low. On the other hand, when the stimulus period T_S is too short compared to the time constant τ, then the difference between the Q_2 and Q_1 decreases, resulting again in low ratio F. That means, that there is a certain range of time constants $\langle \tau_{min}, \tau_{max} \rangle$ for which the described algorithm will work when given a fixed stimulus period T_S and minimal ratio F_{min}. Solving the equivalent circuit of the whole-cell configuration (Fig. 1E), an exact relation for the ratio F can be derived and after rearranging the expression for the minimal and maximal value of the time constant is obtained:

$$\tau_{min} = \frac{T_S\,(F_{min} - 1)}{8} \cdot \frac{R_S}{R_M} \tag{5}$$

$$\tau_{max} = \frac{T_S}{4 \cdot \ln\,(F_{min} + 1)} \tag{6}$$

where R_M and R_S are the membrane and series resistances (Fig. 1). Assuming $T_S = 20$ ms, $F_{min} = 3$ and $R_M/R_S = 100$, the algorithm should be able to successfully identify the exponential response with a time constant raging from 50 μs to 3.6 ms. This range should cover a wide variety of cell types from small chromaffin cells to large myocytes. Using Eqs. (5) and (6), the range of time constants can be shifted and narrowed to be suitable for any specific type of cells.

A state machine for automated whole-cell patch-clamp

Combining the theoretical analysis described above with practical experience from real patch-clamp experiments on rat ventricular myocytes, we designed a finite state machine that may serve for assistance or automation of individual tasks related to formation of the whole-cell configuration. The function of the state machine is described by the state diagram in Fig. 3. The machine may exist in five operating states ("In air", "In bath", "On cell", "Gigaseal" and "Whole-cell"), three error states ("Lost seal", "Lost cell" and "Broken pipette") and one temporary state "Measure R_{pipette}" that is in fact a sub-state of "In bath". The starting state is "In air". Transitions between individual states are defined by the type of current response (exponential decay or square wave) determined using Eqs. (1–3) and values of the air, pipette or seal resistance (Eq. (4)). Once the system gets into any of the three error states, it stays there until the user-operated restart to allow,

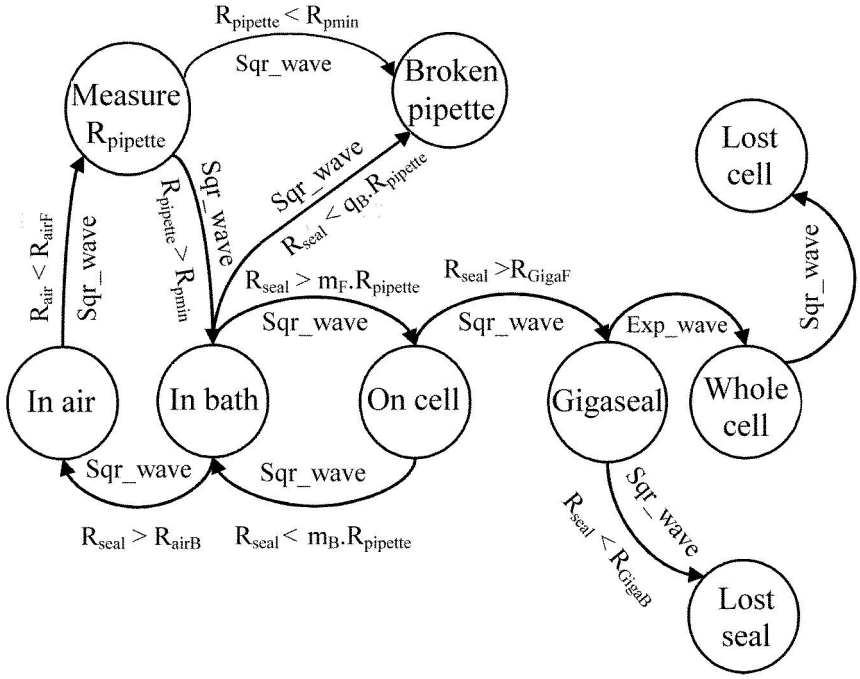

Figure 3. The state diagram of the finite state machine for automated whole-cell patch-clamp. Circles illustrate all possible states in which the state machine may exist. Transitions between the states may occur only in direction indicated by arrows and only when conditions stated near the arrows are fulfilled. Parameters defining in these conditions are explained in Table 1 together with their default values for experiments on rat ventricular myocytes. Required type of current response for each transition is indicated as Sqr_wave (square wave response) or Exp_wave (exponential wave response).

for instance, unlimited time for replacement of the patch-pipette and/or exchange of the cell suspension. Critical values of parameters defining transitions between states summarized in Table 1 were determined empirically and verified in more than 50 patch-clamp experiments on rat ventricular myocytes. To suppress the influence of experimental noise, every transition condition has to be fulfilled in at least five consecutive measurement cycles before it is accepted. For substantially different cell type, patch pipette construction or experimental conditions, the relevant parameters of the state machine should be set properly. Representations of the operating and error states and definitions of state transitions were designed primarily with the "whole-cell" recording mode as the target configuration. The patch-clamp technique offers another three recording modes: the "cell-attached" mode, which is equivalent to the "Gigaseal" state, and the "inside-out" and "outside-out" modes, which are similar to the "Gigaseal" state. Depending on the value of seal resistance after inadvertent detaching of the pipette from the cell the state machine remains in the "Gigaseal" state or switches to "Lost seal" state. In case that correct identification of "inside-out" and "outside-out" modes was required, it would be necessary to define a new state "Cell-free patch", which can be connected to the "Lost seal" state or the "Lost cell" state if the seal resistance $R_{\mathrm{seal}} > \mathrm{R_{GigaF}}$ (see Table 1), and a square wave current response was detected (not presented).

The state machine was implemented and tested with the Digidata 1320A acquisition system on IBM PC running MS Windows (Figs. 4, 5). This implementation assisted the experimenter by issuing different sound alerts at different states of the experiment and by automatic setting of proper values of the holding potential and amplitude of the square wavestimulus generated by the software, while letting

Table 1. Parameters determining transitions of the state machine

Parameter	Description	Default value
R_{airF}	threshold value required for acceptance of transition to "In bath" state	20 MΩ
R_{airB}	threshold value required for acceptance of transition back to "In air" state	700 MΩ
R_{pmin}	required minimal value of R_{pipette}	1 MΩ
q_{B}	coefficient for identification of "Broken pipette" state	0.75
m_{F}	coefficient for acceptance of transition to "On cell" state	2
m_{B}	coefficient for acceptance of transition back to "In bath" state	1.5
R_{GigaF}	minimal R_{seal} value for acceptance of transition to "Gigaseal" state	700 MΩ
R_{GigaB}	minimal R_{seal} value required to stay in "Gigaseal" state	350 MΩ

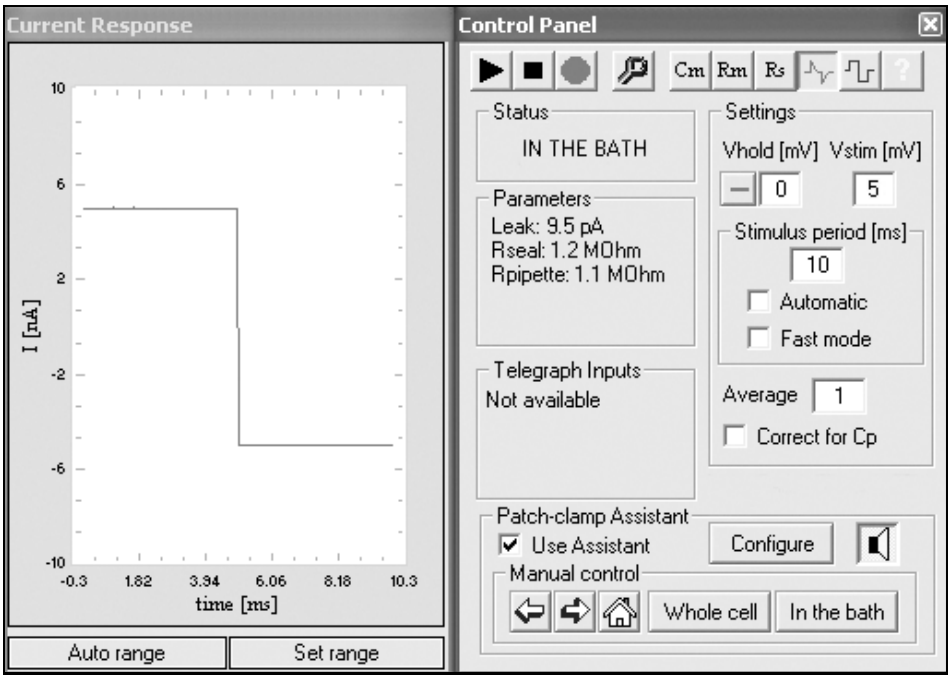

Figure 4. The main dialog window of the software. Current recording state automatically identified by the state machine is indicated in the "Status" box. Electrical parameters of the current recording state such as the pipette resistance, seal resistance, etc. are displayed below, in the "Parameters" box. Basic controls of the state machine for automated patch-clamp useful during the experiment are enclosed in the "Patch-clamp Assistant" box. The user has a possibility to manually proceed to the next or previous recording state, or directly switch to "In the bath" or "Whole-cell" state. Configuration of the "Patch-clamp Assistant" can be modified upon pushing the button "Configure" (see Fig. 5).

him free to concentrate on micromanipulations or other maneuvers occupying his attention. The experimenter has a possibility to manually proceed to the next or previous state or directly jump to the "Whole-cell" or "In bath" states in case of erroneous recognition of the state by the state machine (Fig. 4). Finally, the binary state of digital outputs of the Digidata 1320A can be set for every single recording state separately to allow automated control of external devices (Fig. 5). For example, three digital outputs can be assigned to a system for automated control of pipette pressure such as the one described by Heyward and Shipley (2003) and the fourth digital output can be used for switching off the z-drive of an electronic micromanipulator when the pipette touches the membrane surface ("On the cell" state) or the bottom of measuring chamber ("Broken pipette" state) (Fig. 5). Although the system was designed for the Digidata 132X (Axon Instruments Inc., Union City, CA) acquisition systems, the state machine itself was written as a self-

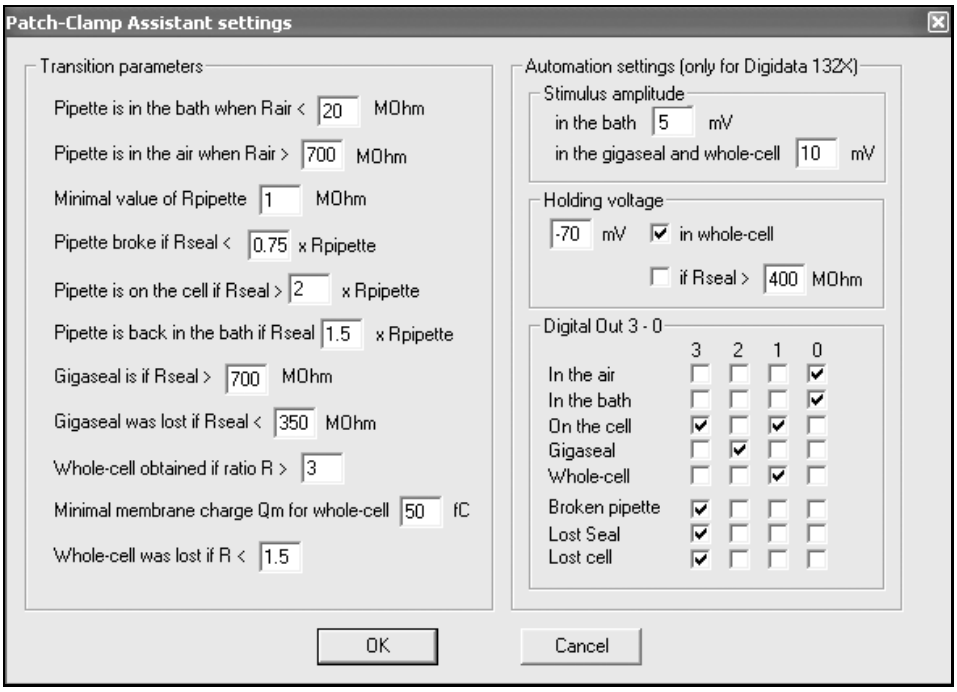

Figure 5. Dialog window with configuration parameters of the "Patch-clamp Assistant". All transition parameters of the state-machine for automated patch-clamp can be modified to better suit for any cell and experiment type. It is possible to set required stimulus amplitude and holding potential levels, which are automatically applied upon successful recognition of the relevant recording state. Every recording state can be assigned a particular 4-bit binary combination available at the four digital outputs on the front panel of the Digidata 132X for automated control of external devices. In the given example, switching on the output 0 connects pipette interior to a source of positive pressure, the output 1 to a source of negative pressure and the output 2 to a source of atmospheric pressure. Switching the output 3 blocks the z-drive of an electronic micromanipulator.

standing C^{++} class "CPatchClampAssistant" independent of current acquisition system. Basically, only the sampled current response in a form of binary data array, together with the stimulus amplitude, stimulus period, current output scaling and sampling frequency is required to run the software state machine properly. The source code of the "CPatchClampAssistant" is available on request.

Discussion

According to our knowledge, this is the first report describing details of automated control of making the conventional glass pipette-based whole-cell patch-clamp. Previous reports of automated patch-clamp were oriented mostly to systems for high-

throughput drug development research using special planar electrodes (Fertig et al. 2002; Klemic et al. 2002; Stett et al. 2003; Asmild et al. 2003) that due to their high cost are not very suitable for basic patch-clamp research. We describe here the state machine that provides automation of and assistance with formation of the whole-cell patch-clamp configuration, designed with consideration of a typical patch-clamp setup of basic-research oriented laboratories. The procedure of formation of the whole-cell configuration was decomposed into several operating and error states according to specific tasks required during the procedure. Transition between individual virtual states of the state machine may serve for generation of control signals for specific tasks, such as changing the direction of internal pipette pressure, stopping the z-drive of an electronic micromanipulator, changing the holding potential, changing the amplitude of the square wave voltage stimulus, etc. All these tasks are usually performed by the experimenter using several specialized devices – the micromanipulator, the pressure system, the patch-clamp amplifier and the digital data acquisition system. Our state machine running on a PC with a suitable A/D and D/A interface is able to support or even to substitute to a large extent the controlling role of the experimenter and to concentrate all operations at the same location – the monitor of a PC – provided that all specialized devices offer some external control. The state machine described here could be a perfect companion to the recently published device for automated control of internal pipette pressure (Heyward and Shipley 2003). With just a little effort this device for pressure control can be controlled by external electrical signals generated by our state machine. Even if devices used for patch-clamp do not offer external control, our state machine may assist in the course of formation of the whole-cell configuration by generating sound alerts indicating events such as the pipette immersed in the bath, pipette touching the cell, or rupturing of the patch, and so freeing the experimenter from frequent checking of the shape of current response and the value of seal resistance. The state machine described here would be greatly appreciated by newcomers in the field mastering the whole-cell patch-clamp technique.

Acknowledgements. We thank to A. Zahradníková for expert comments on the manuscript. This work was supported by APVT-51-031104 and VEGA 2/4153/24.

References

Asmild M., Oswald N., Krzywkowski K. M., Friis S., Jacobsen R. B., Reuter D., Taboryski R., Kutchinsky J., Vestergaard R. K., Schroder R. L., Sorensen C. B., Bech M., Korsgaard M. P., Willumsen N. J. (2003): Upscaling and automation of electrophysiology: toward high throughput screening in ion channel drug discovery. Recept. Channels **9**, 49—58

Fertig N., Blick R. H., Behrends J. C. (2002): Whole cell patch clamp recording performed on a planar glass chip. Biophys. J. **82**, 3056—3062

Hamill O. P., Marty A., Neher E., Sakmann B., Sigworth F. J. (1981): Improved patch-clamp techniques for high-resolution current recording from cells and cell-free membrane patches. Pflügers Arch. **391**, 85—100

Heyward P. M., Shipley M. T. (2003): A device for automated control of pipette internal pressure for patch-clamp recording. J. Neurosci. Methods **123**, 109—115

Klemic K. B., Klemic J. F., Reed M. A., Sigworth F. J. (2002): Micromolded PDMS planar electrode allows patch-clamp electrical recordings from cells. Biosens. Bioelectron. **17**, 597—604

Lepple-Wienhues A., Ferlinz K., Seeger A., Schafer A. (2003): Flip the tip: an automated, high quality, cost-effective patch clamp screen. Recept. Channels **9**, 13—17

Stett A., Burkhardt C., Weber U., van Stiphout P., Knott T. (2003): CYTOCENTERING: a novel technique enabling automated cell-by-cell patch clamping with the CYTOPATCH chip. Recept. Channels **9**, 59—66

Zahradnikova A., Kubalova Z., Pavelkova J., Gyorke S., Zahradnik I. (2004): Activation of calcium release assessed by calcium release-induced inactivation of calcium current in rat cardiac myocytes. Am. J. Physiol., Cell. Physiol. **286**, C330—341

Final version accepted: June 6, 2005